Published in final edited form as:
Microb Pathog. 2008 July ; 45(1): 70–78.

Verification and dissection of the *ospC* operator by using *flaB* promoter as a reporter in *Borrelia burgdorferi*

Qilong Xu, **Kristy McShan**, and **Fang Ting Liang***
Department of Pathobiological Sciences, Louisiana State University, Baton Rouge, Louisiana 70803, USA

Abstract

The Lyme disease spirochete *Borrelia burgdorferi* must repress expression of outer surface protein C (OspC) to effectively evade specific humoral immunity and to establish persistent infection. This ability largely relies upon a regulatory element, the only operator that has been reported in spirochetal bacteria. Immediately upstream of the *ospC* promoter, two sets of inverted repeats (IRs) constitute small and large palindromes, in which the right IR of the large palindrome contains the left IR of the small one, and may collectively function as the *ospC* operator. In the study, the large palindrome with or without the small IR was fused with a *flaB* promoter, which was used to drive expression of a promoterless *ospC* copy as a reporter gene, and introduced into OspC-deficient *B. burgdorferi*. The presence of the large palindrome alone significantly reduced *ospC* expression driven by the fused *flaB* promoter in the joint tissue of severe combined immunodeficiency (SCID) mice, and rescued spirochetes from elimination by passively transferred OspC antibody in infected SCID mice and specific immune responses elicited in immunocompetent mice, confirming a function of the IRs as an operator. Inclusion of the small IR further enhanced the ability of the large palindrome to reduce the activity of the fused *flaB* promoter, indicating that the small IR is a part of the operator. Taken together, the study led to successful verification and dissection of the *ospC* operator.

Keywords

Bacterial pathogenesis; Gene regulation; Lyme disease

1. Introduction

The Lyme disease spirochete, *Borrelia burgdorferi*, is one of the most invasive bacterial pathogens, causing persistent infection despite the development of vigorous immune responses [1,2]. Tight regulation of outer surface protein (Osp) expression is crucial for its pathogenic strategy. The pathogen abundantly expresses OspA/B in the unfed tick [3–6], consistent with an important role of these lipoproteins in spirochetal persistence in the vector [7,8]. A fresh blood meal down-regulates OspA/B and up-regulates OspC and others, a process that prepares *B. burgdorferi* for infection of mammals, regardless of whether OspC is required for salivary gland invasion [9–12]. Repression of OspA/B expression in mammals is critical for the maintenance of the enzootic cycle because their expression would ultimately induce a strong humoral response and, as a result, may effectively block acquisition of *B. burgdorferi* by the

*Corresponding author. Tel.: +1 225 578 9699; Fax: +1 225 578 9701. E-mail address: fliang@vetmed.lsu.edu (F.T. Liang).

vector [13–15], regardless of whether OspA/B can be targeted by borreliacidal antibodies in mammalian tissues [16]. *B. burgdorferi* abundantly expresses OspC only during early infection when the antigen has an important role and before specific humoral responses have developed [17–19]. OspC is not only a strong immunogen but also an effective target of protective immunity; its expression induces a robust humoral response that imposes tremendous pressure on the pathogen [20,21]. To cause persistent infection, *B. burgdorferi* must down-regulate OspC [17,18,22,23]. If *B. burgdorferi* fails to repress OspC expression or undergo escape mutations on the *ospC* gene, infection would be cleared [20]. It is also crucial for *B. burgdorferi* to keep the *ospC* gene off after it is acquired by the tick vector as OspC antibodies in blood meal may kill spirochetes expressing the antigen in the vector [24], leading to discontinuation of the enzootic cycle.

Only three σ factors can be identified from the entire genome of *B. burgdorferi*, including the major factor, RpoD (σ^{70}), and two alternative factors, RpoN (σ^{54}) and RpoS (σ^{38}) [25]. Moreover, the two alternative factors compose a regulatory network, in which RpoS expression depends on RpoN [26,27], greatly limiting their role in contribution to diverse gene regulation. In the unfed tick, the network is silent, so are the RpoS-dependent genes, such as *ospC*, decorin-binding proteins A/B (*dbpA*/*B*), *ospF* and *bbk32* [3,28–30]. During mammalian infection, *B. burgdorferi* apparently mobilizes all the three σ factors [31–33]; therefore, selective gene down-regulation must depend on mechanisms other than controlling expression of these factors.

The identification of the *ospC* operator helps interpret the ability of *B. burgdorferi* to selectively down-regulate *ospC*, while actively transcribing other RpoS-dependent genes during mammalian infection [34]. While the regulatory element remains to be verified in a different system, two sets of inverted repeats (IRs) immediately upstream of the *ospC* promoter constitute small and large palindromes, in which the right IR of the large palindrome contains the left IR of the small one, and may collectively function as an operator but have to be confirmed. Although *ospC* is probably the most investigated among genes in spirochetal bacteria, the full *ospC* promoter region remains to be defined even after attempts from two leading groups in the field [35,36]. In contrast, the *flaB* promoter is a well defined σ^{70}-dependent promoter, driving constitutive gene expression [37]. In the study, the large palindrome with or without the small right IR was fused with the *flaB* promoter, which was used to drive expression of a promoterless *ospC* copy as a reporter gene, and introduced into OspC-deficient *B. burgdorferi*. The study allowed us to successfully verify and dissect the *ospC* operator.

2. Results

2.1. Identification of a minimum *flaB* promoter

The efficiency for the *ospC* operator to repress the activity of a downstream promoter is likely position-dependent, so unessential upstream sequences of the *flaB* promoter should be removed. To identify a minimum *flaB* promoter, two constructs containing the identical promoterless *ospC* copy as a reporter gene were used. The construct pBBE22-*flaBp*$_{min}$-*ospC*, which was created as illustrated in Fig. 1A&B, harbored a *flaB* promoter sequence extending just to the -35 region, consequently called a minimum promoter; while pBBE22-*ospC*′ constructed in our previous study [20], contained a *flaB* promoter extending to −192 from the transcriptional start site and was expected to drive maximum transcriptional activity. The feature of the constructs was summarized in Table 1.

The two constructs were electroporated into the *ospC* mutant, which was generated and characterized in our previous study [34]; 16 and 18 transformants were obtained from the transformation with each construct. Plasmid analyses identified two clones receiving each

construct, namely *Bp-C*/1, *Bp-C*/2, *ΔospC*/*ospC′*/1, and *ΔospC*/*ospC′*/2. The clones *Bp-C*/1and *Bp-C*/2 received pBBE22-*flaBp*$_{min}$-*OspC*, while the clones *ΔospC*/*ospC′*/1 and *ΔospC*/*ospC′*/2 obtained pBBE22-*ospC′*. These clones shared the same plasmid content as the *ospC* mutant, which lost lp25, lp5, lp21 and cp9 [34]. OspC expression resulting from introduction of the constructs was confirmed by immunoblot analysis (Fig. 1C), demonstrating that both constructs actively drove *in vitro* OspC expression.

To more precisely compare the activity of the constructs to drive reporter expression, the *Bp-C*/1, *Bp-C*/2, *ΔospC*/*ospC′*/1, and *ΔospC*/*ospC′*/2 spirochetes were harvested at early log and stationary phase. RNA was prepared and analyzed for *ospC* and *flaB* mRNA accumulation by RT-qPCR. At early log phase, introduction of the constructs pBBE22-*ospC′* and pBBE22-*flaBp*$_{min}$-*ospC* led to the accumulation of 2049 and 1926 *ospC* transcripts, respectively, to match every 1000 *flaB* mRNA copies (Fig. 2A), indicating that the two promoter versions initiated reporter expression as equally well ($P = 0.26$). At stationary phase, the minimum *flaB* promoter drove *ospC* transcription also as effectively as the long promoter version ($P = 0.47$); although the two constructs increased *ospC* mRNA copies to 5281 and 5137, respectively, for every 1000 *flaB* transcripts produced, representing 2.6- and 2.7-fold increases over early log phase (*P* values were 5.7×10^{-7} and 6.9×10^{-7}, respectively).

To explore how the constructs more effectively increased *ospC* mRNA accumulation at stationary rather than early log phase, the copy numbers of the *kan* gene on the constructs and the chromosomal *flaB* gene were determined by qPCR. As shown in Fig. 2B, *B. burgdorferi* produced, on average, six copies of the constructs to match each copy of the linear chromosome at early log phase and increased to over 40 copies at stationary phase, representing a nearly 7-fold increase ($P = 7.1 \times 10^{-6}$). Compared to a less than 3-fold increase in *ospC* mRNA (Fig. 2A), the fused *flaB* promoter did not more efficiently initiate reporter expression at stationary phase. Instead, increased *ospC* mRNA accumulation during stationary phase apparently resulted from a dramatic rise in copy numbers of the *ospC* gene associated with the shuttle vector per cell.

Next, the activity of the two constructs to initiate *ospC* expression was compared in the murine host. Subgroups of five SCID mice were inoculated with the clones *Bp-C*/1, *Bp-C*/2, *ΔospC*/*ospC′*/1, or *ΔospC*/*ospC′*/2. In all 20 animals, joint swelling evolved around 10 days post-inoculation and developed into severe arthritis within a week (data not shown), indicating that all four clones were infectious. Mice were euthanized one month post-inoculation; RNA was extracted and quantified for *ospC* and *flaB* transcripts. As shown in Fig. 2C, the two constructs led to similar *ospC* mRNA accumulation in the heart ($P = 0.89$), joint ($P = 0.77$), and skin tissue ($P = 0.36$), indicating that the minimum *flaB* promoter initiated reporter expression as efficiently as the full-length promoter.

2.2. The presence of the large palindrome alone is able to effectively reduce the activity of a fused *flaB* promoter in joints of SCID mice but inclusion of the small IR further enhances the ability

Immediately upstream of the *ospC* promoter, two sets of IRs constitute small and large palindromes, in which the right IR of the large palindrome essentially contains the left IR of the small one (Fig. 3A), and may collectively function as the operator. To dissect the regulatory sequence, pBBE22-*Co1-flaBp-ospC*, containing the large palindrome and the small IR, and pBBE22-*Co2-flaBp-ospC*, harboring only the large one, were generated as diagramed in Fig. 3A&B before being electroporated into the *ospC* mutant. Nine and 16 transformants were obtained from the transformation with each construct. Plasmid analyses identified two clones receiving each construct, namely *Co1-Bp-C*/1, *Co1-Bp-C*/2, *Co2-Bp-C*/1 and *Co2-Bp-C*/2. These clones shared the same plasmid content as the *ospC* mutant [34]. Active OspC expression

resulting from the introduction of the constructs was confirmed by immunoblot analysis (Fig. 3C).

To examine whether the presence of the operator versions influences the *in vitro* activity of the fused promoter, the *Co1-Bp-C*/1, *Co1-Bp-C*/2, *Co2-Bp-C*/1 and *Co2-Bp-C*/2 spirochetes were harvested at early log and stationary phases. RNA was prepared and analyzed for *ospC* expression by RT-qPCR. The clones *Bp-C*/1 and *Bp-C*/2 were used as a control. No significant differences were noted in *ospC* mRNA accumulation by the three genotypes either at early log or stationary phase (data not shown), indicating that the presence of the *ospC* operator sequences did not affect the activity of the fused *flaB* promoter when spirochetes were grown *in vitro*.

The ability of the two operator versions to influence the activity of a fused promoter was examined in mice. Subgroups of five SCID mice were inoculated with the clone *Co1-Bp-C*/1, *Co1-Bp-C*/2, *Co2-Bp-C*/1 or *Co2-Bp-C*/2. An additional 10 mice were inoculated with the clone *Bp-C*/1 or *Bp-C*/2 as a control. In all 30 mice, joint swelling evolved around 10 days post-inoculation and developed into severe arthritis within a week (data not shown), indicating that all mice were infected. Animals were euthanized one month post-inoculation for the assessment of *ospC* transcriptional activity. As shown in Fig. 4, incorporation of either *ospC* operator version did not change reporter gene expression in heart ($P > 0.05$) or skin tissue ($P > 0.05$). In the joint, however, the presence of the long operator version reduced *ospC* mRNA accumulation by 44% ($P = 1.9 \times 10^{-7}$), compared with a 22% decline caused by the presence of the short version ($P = 0.05$), indicating that the *ospC* operator is able to effectively reduce the activity of the fused *flaB* promoter in joint tissues and, thus, confirming the function of the *ospC* operator. Moreover, the longer operator reduced *ospC* expression 28% more effectively than the shorter version ($P = 0.02$), indicating that the small IR also contributes to the function of the operator to reduce the activity of the downstream promoter.

2.3. The presence of the large palindrome alone confers the responsiveness of a fused *flaB* promoter to treatment with OspC MAb but inclusion of the small IR further enhances the responsiveness

To further examine the influence of the *ospC* operator on the activity of a fused promoter, subgroups of 10 SCID mice were challenged with the clone *Bp-C*/1, *Bp-C*/2, *Co1-Bp-C*/1, *Co1-Bp-C*/2, *Co2-Bp-C*/1 or *Co2-Bp-C*/2. An additional group of 10 mice were inoculated with the clone *ΔospC*/*FL*/1 as a control. This clone was generated by introducing a full-length *ospC* gene carried by pBBE22 into the *ospC* mutant in our previous study [34]. In all 70 mice, joint swelling evolved around 10 days post-inoculation and developed into severe arthritis within a week (data not shown). At 3 weeks, five mice from each group received 100 μg of either OspC MAb or purified murine IgG as a control. One week later, mice were euthanized; heart, joint, and skin samples were used for bacterial culture. As expected, spirochetes were recovered from each specimen harvested from all of the 35 IgG-treated mice (Table 2). As a positive control, the *ΔospC*/*FL*/1 spirochetes were recovered from all of the joints and most of the heart and skin specimens of the five MAb-treated mice. Transferred MAb cleared infections in each tissue from all 10 mice that had been inoculated with either the clone *Bp-C*/1 or *Bp-C*/2. In contrast, the *Co1-Bp-C*/1, *Co1-Bp-C*/2, *Co2-Bp-C*/1 or *Co2-Bp-C*/2 spirochetes were grown from each of the joints, some of the skin specimens, but none of the heart samples, which were taken from the 20 MAb-treated mice (Table 2). These data indicated that the presence of either operator version provides *B. burgdorferi* with the ability to avoid elimination by the OspC antibody, again, confirming the function of the *ospC* operator.

RNA was extracted from joint specimens harvested from all 35 IgG-treated mice and 25 of the 35 MAb-treated mice, then analyzed for *ospC* and *flaB* mRNA transcripts by RT-qPCR. The clearance of infection excluded 10 mice initially infected with either the clone *Bp-C*/1 or *Bp-*

C/2 and treated with MAb. As previously reported [34], in response to MAb treatment, the *ΔospC*/*FL*/1 spirochetes reduced *ospC* expression by 87-fold ($P = 3.2 \times 10^{-7}$) (data not shown). Consistent with the data presented in Fig. 4, addition of the long and short operator versions led to 41% ($P = 6.2 \times 10^{-6}$) and 21% ($P = 0.03$) reductions, respectively, in *ospC* mRNA accumulation (Fig. 5). MAb treatment further reduced *ospC* expression by 4.5- and 2.5-fold in spirochetes harboring the long ($P = 1.7 \times 10^{-12}$) and the short operator versions ($P = 3.3 \times 10^{-6}$), respectively, indicating that either version reduces the activity of a fused *flaB* promoter in response to treatment with OspC MAb. Furthermore, the long operator version showed a 59% more effectiveness in reducing *ospC* expression than the short one in response to treatment with OspC MAb ($P = 7.1 \times 10^{-6}$), again, indicating that the small IR is also crucial for the function of the operator.

2.4. Verification of the function of the *ospC* operator during chronic infection of immunocompetent mice

Next, the function of the *ospC* operator was further verified in immunocompetent mice. Groups of five BALB/c mice were challenged with the clone *Bp-C*/1, *Bp-C*/2, *Co1-Bp-C*/1, *Co1-Bp-C*/2, *Co2-Bp-C*/1 or *Co2-Bp-C*/2. An additional group of 10 mice were challenged with the clone *ΔospC*/*FL*/1 as a positive control. Ear biopsies taken for bacterial culture at 3 weeks post-inoculation showed that all of the 40 mice were infected (data not shown). Animals were sacrificed 4 months post-inoculation; heart, joint and skin samples were harvested for bacterial isolation. The *ΔospC*/*FL*/1 spirochetes were grown from each of the heart, joint and skin specimens of 10 inoculated mice (Table 3). Although the *Bp-C*/1 and *Bp-C*/2 spirochetes were recovered from most of the skin specimens, they were cleared from the heart and joint tissues of 10 inoculated mice. In contrast, *B. burgdorferi* was grown from each of the skin specimens and most of the heart and joint tissues of 20 mice that had been challenged with the clone *Co1-Bp-C*/1, *Co1-Bp-C*/2, *Co2-Bp-C*/1 or *Co2-Bp-C*/2, indicating that either *ospC* operator version helps *B. burgdorferi* evade the immune system. Therefore, the study successfully verified the function of the *ospC* operator in immunocompetent mice.

3. Discussion

As a σ^{70}-dependent promoter, the *flaB* promoter is one of the most active promoters, which drives constitutive gene expression during the entire enzootic cycle of *B. burgdorferi*. To verify and dissect the newly identified operator of the RpoS-dependent *ospC* gene, the *flaB* promoter was used as a reporter promoter and fused with a promoterless *ospC* as a reporter gene. The study not only verified the function of the *ospC* operator but also demonstrated that all the IRs collectively act as a *cis*-element to influence the activity of a downstream promoter.

Identification of the *ospC* operator predicts the existence of a repressor [34]. However, nothing is known about the regulatory protein or how it is induced during the enzootic cycle of *B. burgdorferi*. *In vitro ospC* expression is always associated with the upregulation of RpoS [26,35,36,38], suggesting that the repressor is not induced *in vitro*. Our previous study showed that deletion of the operator does not influence *in vitro ospC* expression, thus, ruling out the involvement of the operator-repressor system in *ospC* regulation [34]. In the current study, the presence of either *ospC* operator version did not affect the activity of the fused *flaB* promoter to initiate a reporter gene expression in cultivated *B. burgdorferi*, further confirming that the potential repressor is not expressed under *in vitro* conditions.

The current study showed that the copy number of shuttle vectors dramatically increased as spirochetes grew from early log to stationary phase. *B. burgdorferi* produced approximately six copies of the introduced construct to match each copy of the linear chromosome at early log phase and increased to more than 40 copies at stationary phase. This increase in *ospC* gene copy number resulted in a dramatic increase in mRNA accumulation, clearly indicating that

manipulating the copy number of a plasmid can achieve selective regulation of specific genes, a potential strategy for gene regulation that has been ignored in *B. burgdorferi*. However, it should be noted that the constructs were modified from pBBE22 [39], which was derived from cp9 [40]. It remains to be confirmed whether the constructs are replicated and maintained as the endogenous plasmid. It is also interesting to know whether the copy numbers of plasmids change during *in vitro* cultivation and the enzootic cycle of *B. burgdorferi*.

Previous studies showed *B. burgdorferi* exhibiting tissue-differential *ospC* expression, with significantly higher expression in both heart and skin tissues than the joints of SCID mice [17,41]. Recent identification of the *ospC* operator led to a successful interpretation of this differential expression pattern [34]. Deletion of the operator results in a dramatic increase in *ospC* expression in joints, but does not affect expression in either heart or skin tissues, suggesting that the potential repressor is induced only in joints of SCID mice [34]. In the current study, the fused *ospC* operator versions did not affect the activity of the reporter *flaB* promoter either in heart or skin tissues, instead reducing *ospC* expression driven by the fused promoter in the joints of SCID mice, indicating the repressor is expressed only in this specific type of tissue in the absence of specific humoral pressure and allowing successful verification of the function of the operator. Because the long version showed more effectiveness in reducing *ospC* expression, the study also led to dissection of the operator. It remains to be determined whether the copy number of the constructs is tissue-dependent or changes during the course of infection. However, these factors should not affect our data interpretations because all our constructs should behave in similar manners under each specific condition.

The biological significance for the existence of the *ospC* operator in *B. burgdorferi* is to confer the ability to evade specific humoral immunity. Previous studies showed that OspC antibodies administered to immunodeficient mice or the specific humoral response induced during infection of immunocompetent mice constitute an overwhelming force to reduce *ospC* expression to a baseline level in all tissues [17,18,22,23]. A recent study also showed that lack of the operator allows the *ospC* promoter to drive constitutive gene expression in all tissues and, as a result, completely diminishes the ability of *B. burgdorferi* to evade specific humoral immunity [34]. In the current study, lack of the operator allowed the fused *flaB* promoter to drive constitutive *ospC* expression in all tissues of SCID mice and, as a consequence, diminished the ability to evade specific OspC antibody. Addition of the operator to the upstream of the *flaB* promoter allowed *B. burgdorferi* to effectively evade clearance by OspC MAb in the joint tissue, an ability that was gained apparently through the down-regulation of *ospC* expression. Because the long operator version conferred *B. burgdorferi* a higher responsiveness to treatment with OspC antibody, the study, again, not only verified the function of the operator but also led to a successful dissection of the operator. The involvement of the fused *ospC* operator was unable to rescue *B. burgdorferi* from elimination by the administration of OspC MAb in the heart tissue, speculating that the sudden presence of specific antibody in a large quantity overwhelmed spirochetes before the down-regulation of *ospC* expression driven by the fused promoter could occur. This explanation is supported by our chronic infectivity study conducted in immunocompetent mice, showing *B. burgdorferi* that was given the operator was grown from most heart specimens collected 4 months after initial inoculation.

Although *B. burgdorferi* with constitutive *ospC* expression driven by a fused *flaB* promoter was eradicated by OspC MAb from all tissues of infected SCID mice, this genotype was able to persist in the skin of immunocompetent mice. Our previous study showed that spirochetes with increased OspC expression via the introduction of an extra *ospC* copy fused with a *flaB* promoter are cleared from all tissues of infected immunocompetent mice, unless escape mutations occur on the constitutively expressed copy [20]. Different *ospC* expression levels might cause this discrepancy. In the previous study, two *ospC* copies, the native gene and the introduced copy, might lead to higher OspC expression, making the pathogen more vulnerable

to specific humoral immunity. This interpretation is supported by our other study [34], in which robust *ospC* expression driven by the *ospC* promoter without control of its operator completely abrogates the ability of *B. burgdorferi* to persist in immunocompetent mice.

During a transcriptional initiation, the σ factor of a RNA polymerase holoenzyme mediates the initial interaction of the polymerase with a specific promoter. Binding of a repressor to its operator may block the interaction, thus preventing a transcriptional initiation. In a bacterium, the same RNA polymerase can use all σ factors the cell expresses, albeit it may exhibit various utilization efficiencies for different σ factors. In addition, the concentration of a specific σ factor in the cell and its ability to mediate the interaction with a target promoter may affect the efficiency of an operator to influence transcriptional initiation. All of these might collectively contribute to the reduced effectiveness of the *ospC* operator to influence the activity of the fused σ^{70}-dependent *flaB* promoter observed in the current study.

A palindromic sequence may form a cruciform structure that interacts with a regulatory protein with high affinity. There are two sets of IRs, potentially forming small and large cruciform structures immediately upstream of the *ospC* promoter (Fig. 3A). However, because the right IR of the large palindrome contains the left IR of the small palindrome, it is unclear how these four IRs are arranged to form secondary and tertiary structures. Our previous study clearly showed that the large palindrome is required for the operator's activity; in the native promoter-operator system, however, we have not been able to address whether the small one contributes to the repressing activity [34]. In the current study, the *ospC* promoter was replaced, allowing us to dissect the operator without the influence of the native promoter. The study showed that although the large palindrome alone was able to effectively reduce the activity of the fused *flaB* promoter, the involvement of all the four IRs significantly improved the repressing activity. In our previous study, deletion of the sequence immediately upstream of the large palindrome has little effect on the activity of the operator, but removal of the left IR of the palindrome completely diminishes the operator's function [34]. Taken together, these studies demonstrate that the operator includes all the four IRs.

4. Materials and methods

4.1. Construction of pBBE22-*flaBp*$_{min}$-*ospC*

As illustrated in Fig. 1, an 883-bp fragment was PCR (polymerase chain reaction) amplified with the use of primers P1F and P1R (Table 4), and of pBBE22-*ospC′* as a template; digested with *Bam*HI and *Xba*I; purified; and cloned into pBBE22 (a gift from S. Norris) [39] after the vector was digested with the same restriction enzymes. The recombinant plasmid pBBE22-*ospC′* was constructed from pBBE22 in our previous study [20]. The insert within pBBE22-*flaBp*$_{min}$-*ospC* was sequenced to ensure that the insert and its flanking sequences were arranged as designed.

4.2. Construction of pBBE22-*Co1-flaBp-ospC* and pBBE22-*Co2-flaBp-ospC*

As illustrated in Fig. 3, 238-bp and 219-bp fragments, namely *Co1* and *Co2*, were PCR amplified with the use of two reverse primers, P2R and P3R (Table 4), respectively, and a common forward primer, P2F, and of borrelial DNA as a template. A third fragment, designated *flaBp-ospC*, was generated by PCR using the primers P3F and P4R, and the construct pBBE22-*flaBp*$_{min}$-*OspC* as a template. After digestion with *Eco*RI and subsequent purification, the fragments *Co1* and *Co2*, respectively, were fused with *flaBp-ospC*. Resulting fragments were used as templates and PCR amplified with the use of primers P4F and P1R, generating *Co1-flaBp-ospC* and *Co2-flaBp-ospC*, respectively. After digestion with *Bam*HI and *Xba*I plus subsequent purification, the two fragments were cloned into pBBE22 after the vector was digested with the same enzymes, completing the construction of pBBE22-*Co1-flaBp-ospC* and

pBBE22-*Co2-flaBp-ospC*, which were then sequenced to ensure that the inserts and their flanking sequences were arranged as designed.

4.3. Transformation of *B. burgdorferi* and selection of transformants

Constructs were electroporated into the *ospC* mutant, which was generated and characterized in our previous study [34]; resulting transformants were screened as described previously [42]. Selected transformants were first surveyed for the presence of lp28-1 as this plasmid is essential for infection of an immunocompetent host [42,43]. Only clones that contained lp28-1 were further analyzed for plasmid content as described previously [42]. Selected clones were grown to late-log phase in Barbour-Stoenner-Kelly H (BSK-H) complete medium at 33°C (Sigma Chemical Co., St. Louis, MO), and subjected to immunoblot analysis probed with a mixture of FlaB and OspC monoclonal antibodies (MAbs), as described previously [20].

4.4. *In vitro* characterization of transformants

Transformants were grown in BSK-H complete medium to middle log and stationary phase at 33°C, and harvested by centrifugation. RNA samples were prepared and quantified for the cDNA copy numbers of *flaB* and *ospC* by reverse transcription-quantitative PCR (RT-qPCR) as previously described [17].

4.5. SYBR green qPCR analysis of *kan* and *flaB* gene copy numbers

Spirochetes were grown and harvested as described above; DNA was extracted using tissue DNA columns per the manufacturer's instruction (Sigma). The copy numbers of the borrelial linear chromosome and the constructs were quantified by using the primers P5F and P5R or P6F and P6R (Table 4) specific for the genes *flaB* and *kan*, respectively. The recombinant plasmids pNCO1T-*actin-flaB*, which was constructed previously [42], and pBBE22 were used as DNA concentration standards for *flaB* and *kan*, respectively. Purified plasmids were determined for DNA concentrations by measuring the optical density at 260 nm wavelength, converted to copy numbers and 10-fold serially diluted within a range of $10^2 – 10^7$ DNA copies/μl. The iTaq SYBR Green Supermix with ROX (Bio-Rad Laboratories, Hercules, CA) and the ABI PRISM™ 7900 sequence detection system (Applied Biosystems, Foster City, CA) were used for qPCR assays. Amplification was performed in a final volume of 10-μl on the ABI PRISM™ 384-well clear optical reaction plate (Applied Biosystems). Two sets of 12 wells on each plate were run for either *flaB* or *kan* DNA concentration standards. Both standards and samples were amplified in duplicate wells. A PCR program with the following parameters was used: 50°C for 2 min; 95°C for 5 min; 40 cycles of 95°C for 20 sec, 60°C for 1 min. The mean DNA copy numbers of *flaB* and *kan* in each sample were calculated from duplicate wells. Data were expressed as the copy number of *kan* per 1000 *flaB* copies.

4.6. Mouse infection study

SCID mice (BALB/c background; ages, 4 -- 8 weeks; provided by the Division of LSU Laboratory Animal Medicine) were given one single intradermal/subcutaneous injection of 10^4 spirochetes. Animals were examined for the development of arthritis at 2-day intervals, starting at day 7, and sacrificed one month post-inoculation. Joint, heart, and skin specimens were collected for RNA preparation. RNA was converted to cDNA and quantified for the mRNA copy numbers of *flaB* and *ospC* by qPCR as described previously [20].

4.7. Passive immunization of infected SCID mice

BALB/c SCID mice were inoculated and monitored for the development of arthritis as described above. Infected mice received a single subcutaneous injection of 100 μg of OspC MAb or purified mouse IgG as a control 3 weeks post-inoculation, as described previously [34]. Mice were sacrificed 1 week after passive immunization; heart, tibiotarsal joint, and skin

specimens were aseptically collected for spirochete culture as previously described [42]. RNA was extracted from joint samples, and used for *ospC* expression analyses as described above.

4.8. Chronic infectivity study

Groups of five to 10 BALB/c mice (ages, 4 -- 8 weeks; provided by the Division of LSU Laboratory Animal Medicine) were given one single intradermal/subcutaneous injection of 10^4 spirochetes. Ear biopsies were conducted for bacterial isolation 3 weeks after inoculation. Mice were euthanized 4 months post-inoculation; heart, tibiotarsal joint and skin specimens were aseptically collected for spirochete culture as previously described [42].

4.9. Statistical analysis

qPCR Data were analyzed by using a one-way analysis of variance (ANOVA), followed by a two-tailed Student *t* test to compare two treatments and calculate *P* values. Data obtained from infection studies were analyzed by using Fisher's exact test. Calculated *P* values of ≤ 0.05 were considered significant.

Acknowledgements

We thank S. Norris for providing pBBE22, P. Rosa for critically reading the manuscript, and M. Kearney for assistance with statistical analysis.

This work was supported in part by a career development award and a grant from NIH/NIAMS, an Arthritis Foundation Investigators award, and P20RR020159 (PI, Kousoulas) from NIH/NCRR.

References

1. Seiler KP, Weis JJ. Immunity to Lyme disease: protection, pathology and persistence. Curr Opin Immunol 1996;8:503–9. [PubMed: 8794009]
2. Steere AC. Lyme disease. N Engl J Med 2001;345:115–25. [PubMed: 11450660]
3. Schwan TG, Piesman J, Golde WT, Dolan MC, Rosa PA. Induction of an outer surface protein on *Borrelia burgdorferi* during tick feeding. Proc Natl Acad Sci U S A 1995;92:2909–13. [PubMed: 7708747]
4. Schwan TG, Piesman J. Temporal changes in outer surface proteins A and C of the Lyme disease-associated spirochete, *Borrelia burgdorferi*, during the chain of infection in ticks and mice. J Clin Microbiol 2000;38:382–8. [PubMed: 10618120]
5. Ohnishi J, Piesman J, de Silva AM. Antigenic and genetic heterogeneity of *Borrelia burgdorferi* populations transmitted by ticks. Proc Natl Acad Sci U S A 2001;98:670–5. [PubMed: 11209063]
6. de Silva AM, Telford SR 3rd, Brunet LR, Barthold SW, Fikrig E. *Borrelia burgdorferi* OspA is an arthropod-specific transmission-blocking Lyme disease vaccine. J Exp Med 1996;183:271–5. [PubMed: 8551231]
7. Yang XF, Pal U, Alani SM, Fikrig E, Norgard MV. Essential role for OspA/B in the life cycle of the Lyme disease spirochete. J Exp Med 2004;199:641–8. [PubMed: 14981112]
8. Neelakanta G, et al. Outer surface protein B is critical for *Borrelia burgdorferi* adherence and survival within *Ixodes* ticks. PLoS Pathog 2007;3:e33. [PubMed: 17352535]
9. Fingerle V, Goettner G, Gern L, Wilske B, Schulte-Spechtel U. Complementation of a *Borrelia afzelii* OspC mutant highlights the crucial role of OspC for dissemination of *Borrelia afzelii* in *Ixodes ricinus*. Int J Med Microbiol 2007;297:97–107. [PubMed: 17267282]
10. Grimm D, et al. Outer-surface protein C of the Lyme disease spirochete: a protein induced in ticks for infection of mammals. Proc Natl Acad Sci U S A 2004;101:3142–7. [PubMed: 14970347]
11. Stewart PE, et al. Delineating the requirement for the *Borrelia burgdorferi* virulence factor OspC in the mammalian host. Infect Immun 2006;74:3547–53. [PubMed: 16714587]
12. Pal U, et al. OspC facilitates *Borrelia burgdorferi* invasion of *Ixodes scapularis* salivary glands. J Clin Invest 2004;113:220–30. [PubMed: 14722614]

13. Tsao J, Barbour AG, Luke CJ, Fikrig E, Fish D. OspA immunization decreases transmission of *Borrelia burgdorferi* spirochetes from infected *Peromyscus leucopus* mice to larval *Ixodes scapularis* ticks. Vector Borne Zoonotic Dis 2001;1:65–74. [PubMed: 12653137]
14. Tsao JI, Wootton JT, Bunikis J, Luna MG, Fish D, Barbour AG. An ecological approach to preventing human infection: vaccinating wild mouse reservoirs intervenes in the Lyme disease cycle. Proc Natl Acad Sci U S A 2004;101:18159–64. [PubMed: 15608069]
15. de Silva AM, Fish D, Burkot TR, Zhang Y, Fikrig E. OspA antibodies inhibit the acquisition of *Borrelia burgdorferi* by *Ixodes* ticks. Infect Immun 1997;65:3146–50. [PubMed: 9234767]
16. Strother KO, Hodzic E, Barthold SW, de Silva AM. Infection of mice with Lyme disease spirochetes constitutively producing outer surface proteins A and B. Infect Immun 2007;75:2786–94. [PubMed: 17371860]
17. Liang FT, et al. *Borrelia burgdorferi* changes its surface antigenic expression in response to host immune responses. Infect Immun 2004;72:5759–67. [PubMed: 15385475]
18. Liang FT, Jacobs MB, Bowers LC, Philipp MT. An immune evasion mechanism for spirochetal persistence in Lyme borreliosis. J Exp Med 2002;195:415–22. [PubMed: 11854355]
19. Tilly K, Bestor A, Jewett MW, Rosa P. Rapid clearance of Lyme disease spirochetes lacking OspC from skin. Infect Immun 2007;75:1517–9. [PubMed: 17158906]
20. Xu Q, Seemanapalli SV, McShan K, Liang FT. Constitutive expression of outer surface protein C diminishes the ability of *Borrelia burgdorferi* to evade specific humoral immunity. Infect Immun 2006;74:5177–84. [PubMed: 16926410]
21. Fung BP, McHugh GL, Leong JM, Steere AC. Humoral immune response to outer surface protein C of *Borrelia burgdorferi* in Lyme disease: role of the immunoglobulin M response in the serodiagnosis of early infection. Infect Immun 1994;62:3213–21. [PubMed: 8039891]
22. Liang FT, Nelson FK, Fikrig E. Molecular adaptation of *Borrelia burgdorferi* in the murine host. J Exp Med 2002;196:275–80. [PubMed: 12119353]
23. Crother TR, et al. Temporal analysis of the antigenic composition of *Borrelia burgdorferi* during infection in rabbit skin. Infect Immun 2004;72:5063–72. [PubMed: 15321999]
24. Gilmore RD Jr, Piesman J. Inhibition of *Borrelia burgdorferi* migration from the midgut to the salivary glands following feeding by ticks on OspC-immunized mice. Infect Immun 2000;68:411–4. [PubMed: 10603419]
25. Fraser CM, et al. Genomic sequence of a Lyme disease spirochaete, *Borrelia burgdorferi*. Nature 1997;390:580–6. [PubMed: 9403685]
26. Hubner A, Yang X, Nolen DM, Popova TG, Cabello FC, Norgard MV. Expression of *Borrelia burgdorferi* OspC and DbpA is controlled by a RpoN-RpoS regulatory pathway. Proc Natl Acad Sci U S A 2001;98:12724–9. [PubMed: 11675503]
27. Yang XF, Alani SM, Norgard MV. The response regulator Rrp2 is essential for the expression of major membrane lipoproteins in *Borrelia burgdorferi*. Proc Natl Acad Sci U S A 2003;100:11001–6. [PubMed: 12949258]
28. Hagman KE, et al. Decorin-binding protein A (DbpA) of *Borrelia burgdorferi* is not protective when immunized mice are challenged via tick infestation and correlates with the lack of DbpA expression by *B. burgdorferi* in ticks. Infect Immun 2000;68:4759–64. [PubMed: 10899883]
29. He M, Boardman BK, Yan D, Yang XF. Regulation of expression of the fibronectin-binding protein BBK32 in *Borrelia burgdorferi*. J Bacteriol 2007;189:8377–80. [PubMed: 17873053]
30. Miller JC, von Lackum K, Babb K, McAlister JD, Stevenson B. Temporal analysis of *Borrelia burgdorferi* Erp protein expression throughout the mammal-tick infectious cycle. Infect Immun 2003;71:6943–52. [PubMed: 14638783]
31. Caimano MJ, et al. Analysis of the RpoS regulon in *Borrelia burgdorferi* in response to mammalian host signals provides insight into RpoS function during the enzootic cycle. Mol Microbiol 2007;65:1193–217. [PubMed: 17645733]
32. Fisher MA, et al. *Borrelia burgdorferi* σ^{54} is required for mammalian infection and vector transmission but not for tick colonization. Proc Natl Acad Sci U S A 2005;102:5162–7. [PubMed: 15743918]

33. Caimano MJ, Eggers CH, Gonzalez CA, Radolf JD. Alternate sigma factor RpoS is required for the *in vivo*-specific repression of *Borrelia burgdorferi* plasmid lp54-borne *ospA* and *lp6.6* genes. J Bacteriol 2005;187:7845–52. [PubMed: 16267308]
34. Xu Q, McShan K, Liang FT. Identification of an *ospC* operator critical for immune evasion of *Borrelia burgdorferi*. Mol Microbiol 2007;64:220–31. [PubMed: 17376084]
35. Eggers CH, Caimano MJ, Radolf JD. Analysis of promoter elements involved in the transcriptional initiation of RpoS-dependent *Borrelia burgdorferi* genes. J Bacteriol 2004;186:7390–402. [PubMed: 15489451]
36. Yang XF, et al. Analysis of the *ospC* regulatory element controlled by the RpoN-RpoS regulatory pathway in *Borrelia burgdorferi*. J Bacteriol 2005;187:4822–9. [PubMed: 15995197]
37. Ge Y, Old IG, Saint Girons I, Charon NW. Molecular characterization of a large *Borrelia burgdorferi* motility operon which is initiated by a consensus σ^{70} promoter. J Bacteriol 1997;179:2289–99. [PubMed: 9079915]
38. Gilbert MA, Morton EA, Bundle SF, Samuels DS. Artificial regulation of *ospC* expression in *Borrelia burgdorferi*. Mol Microbiol 2007;63:1259–73. [PubMed: 17257307]
39. Purser JE, Lawrenz MB, Caimano MJ, Howell JK, Radolf JD, Norris SJ. A plasmid-encoded nicotinamidase (PncA) is essential for infectivity of *Borrelia burgdorferi* in a mammalian host. Mol Microbiol 2003;48:753–64. [PubMed: 12694619]
40. Stewart PE, Thalken R, Bono JL, Rosa P. Isolation of a circular plasmid region sufficient for autonomous replication and transformation of infectious *Borrelia burgdorferi*. Mol Microbiol 2001;39:714–21. [PubMed: 11169111]
41. Crother TR, Champion CI, Wu XY, Blanco DR, Miller JN, Lovett MA. Antigenic composition of *Borrelia burgdorferi* during infection of SCID mice. Infect Immun 2003;71:3419–28. [PubMed: 12761126]
42. Xu Q, et al. Association of linear plasmid 28-1 with an arthritic phenotype of *Borrelia burgdorferi*. Infect Immun 2005;73:7208–15. [PubMed: 16239515]
43. Grimm D, et al. Experimental assessment of the roles of linear plasmids lp25 and lp28-1 of *Borrelia burgdorferi* throughout the infectious cycle. Infect Immun 2004;72:5938–46. [PubMed: 15385497]
44. Ge Y, Old IG, Girons IS, Charon NW. The *flgK* motility operon of *Borrelia burgdorferi* is initiated by a σ^{70}-like promoter. Microbiology 1997;143(Pt 5):1681–90. [PubMed: 9168617]
45. Marconi RT, Samuels DS, Garon CF. Transcriptional analyses and mapping of the *ospC* gene in Lyme disease spirochetes. J Bacteriol 1993;175:926–32. [PubMed: 7679385]
46. Margolis N, Hogan D, Cieplak W Jr, Schwan TG, Rosa PA. Homology between *Borrelia burgdorferi* OspC and members of the family of *Borrelia hermsii* variable major proteins. Gene 1994;143:105–10. [PubMed: 8200524]

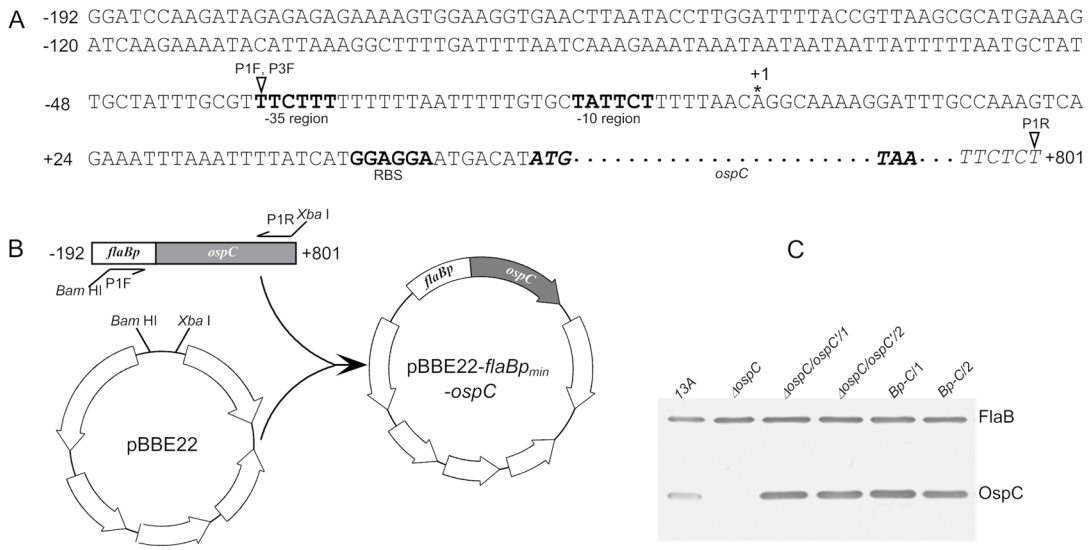

Fig. 1.

Identification of a minimum *flaB* promoter. (A) Extended *flaB* promoter sequence and fused promoterless *ospC* gene. This sequence is already in pBBE22-*ospC′*, which was constructed from pBBE22 in our previous study [20]. The sequence includes the *flaB* promoter and upstream sequence, extending to −192 from its transcriptional start site, and a promoterless *ospC* gene (italic), extending from the start codon ATG (boldface) to +801 from the transcriptional start site of the *ospC* gene. The stop codon TAA (boldface) of *ospC* is also present. The −35 and −10 regions, and the putative ribosome-binding site (RBS) (all in boldface type) of the *flaB* gene are indicated. The asterisk marks the previously identified transcriptional initiation site [44]. The amplification start sites of primers, P1F, P3F and P1R, are pointed with open triangles. P1F and P3F had an identical sequence, but were incorporated with different restriction enzyme sites, and were used for plasmid construction described in this figure and Fig. 3, respectively. (B) Construction of pBBE22-*flaBp*$_{min}$-*ospC* from pBBE22 and pBBE22-*ospC′*. An 883-bp fragment was PCR amplified with the use of primers P1F and P1R, and of pBBE22-*ospC′* as a template, then cloned into pBBE22. (C) Immunoblot analysis of OspC expression. The parental clone 13A, the *ospC* mutant (*ΔospC*), and the clones *ΔospC*/*ospC′*/1, *ΔospC*/*ospC′*/2, *Bp-C*/1 and *Bp-C*/2 were verified for OspC expression by immunoblotting probed with a mixture of FlaB and OspC MAbs.

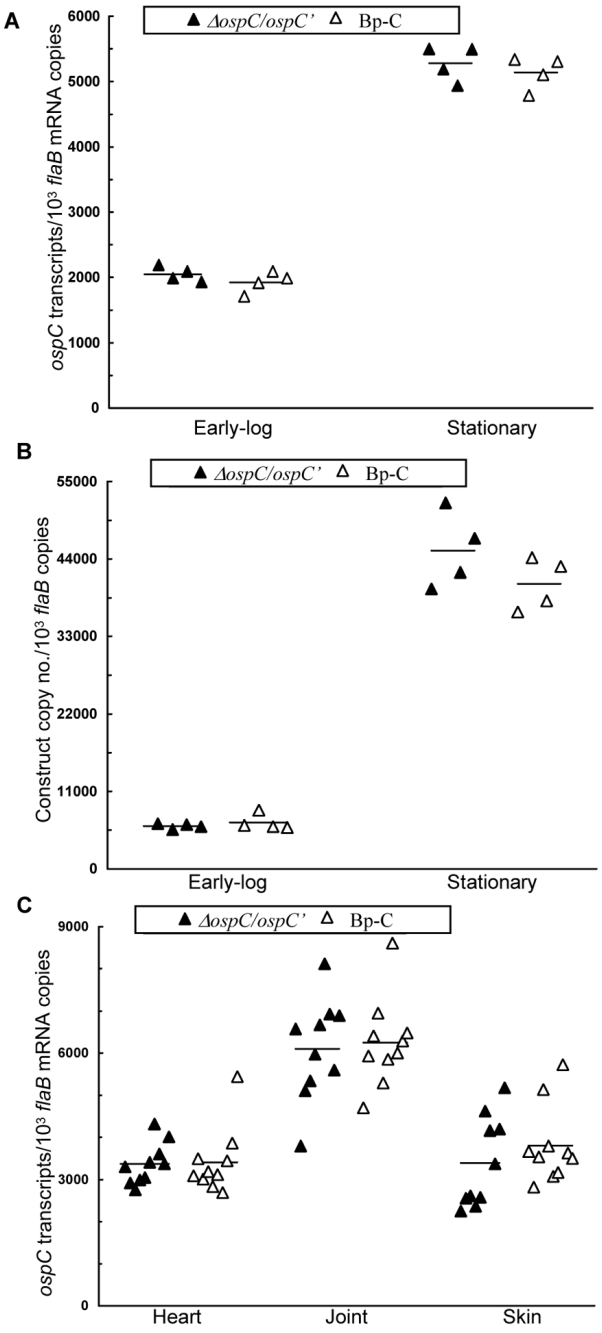

Fig. 2.

The minimum *flaB* promoter drives maximum *in vitro* and *in vivo ospC* expression. (A) The two constructs drive active *in vitro ospC* expression. The *ΔospC*/*ospC'*/1, *ΔospC*/*ospC'*/2, *Bp-C*/1, and *Bp-C*/2 spirochetes were grown, in duplicate, to early log and stationary phase at 33° C. RNA was extracted and analyzed by RT-qPCR for *flaB* and *ospC* mRNA copy numbers. The expression activity is presented as *ospC* mRNA copy numbers per 1000 *flaB* transcripts. Data generated from *ΔospC*/*ospC'*/1and *ΔospC*/*ospC'*/2 were combined and compared with those obtained from *Bp-C*/1 and *Bp-C*/2. (B) *B. burgdorferi* increases accumulation of constructs from early log to stationary phase. DNA was also extracted from spirochetes grown as described above and quantified for *flaB* and *kan* copies. The data are expressed as *kan* DNA

copy numbers per 1000 *flaB* copies. (C) The two constructs drive similar *ospC* expression in mice. Subgroups of five SCID mice were inoculated with the clone *ΔospC*/*ospC′*/1, *ΔospC*/*ospC′*/2, *Bp-C*/1, or *Bp-C*/2. All mice were sacrificed one month later; RNA samples were prepared from the heart, joint and skin specimens and quantified for *flaB* and *ospC* expression by RT-qPCR. The data are presented as *ospC* transcripts per 1000 *flaB* mRNA copies and in two groups by combining the subgroups *ΔospC*/*ospC′*/1 and *ΔospC*/*ospC′*/2, and *Bp-C*/1 and *Bp-C*/2.

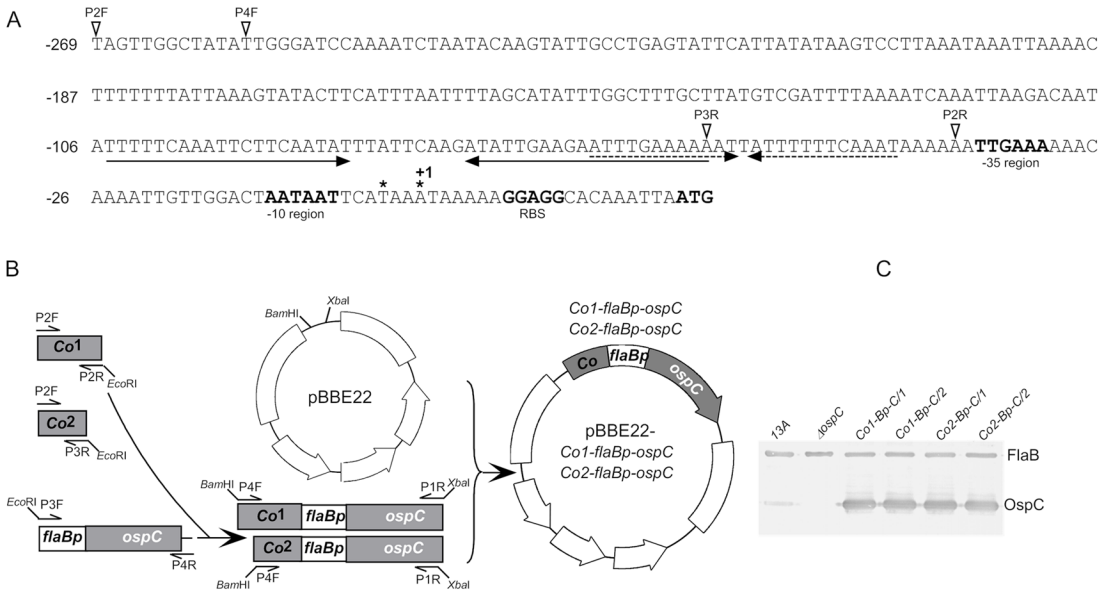

Fig. 3.

Generation of *B. burgdorferi* expressing *ospC* driven by a fused *flaB* promoter under control of the *ospC* operator. (A) The regulatory elements including extended *ospC* promoter and operator. Upstream regions of the *ospC* gene including two large inverted repeats (indicated by a pair of divergent arrows) and two small inverted repeats (indicated by a pair of dashed divergent arrows), the extended −35 and −10 regions, the putative ribosome-binding site (RBS), and the start codon ATG (all in boldface type) are indicated. The asterisks mark two previously identified transcriptional initiation sites [45,46]; the downstream one is designated as +1 because of a larger distance to the −10 region. The amplification starting sites of the four primers, P2F, P4F, P2R and P3R used for vector construction are pointed with open triangles. (B) Construction of pBBE22-*Co1-flaBp-ospC* and pBBE22-*Co2-flaBp-ospC*. Two fragments, *Co1* and *Co2*, were PCR amplified with the use of reverse primers P2R and P3R, respectively, and a common forward primer P2F, and of borrelial DNA as a template. The fragment *flaBp-OspC* was generated by PCR using the primers P3F (see Fig. 1 for the binding site of P3F) and P4R (the binding site of P4R within the construct pBBE222-*flaBp*$_{min}$-*ospC* is not shown) and pBBE22-*flaBp*$_{min}$-*ospC* as a template. The fragments *Co1* and *Co2* were fused with *flaBp-ospC*, forming *Co1-flaBp-ospC* and *Co2-flaBp-ospC*, respectively, amplified by nested PCR with use of the primers P4F and P1R (see Fig. 1 for the binding site of P1R), and cloned into pBBE22. (C) Immunoblot analysis of OspC expression. The parental clone 13A, the *ospC* mutant, and the clones *Co1-Bp-C*/1, *Co1-Bp-C*/2, *Co2-Bp-C*/1, and *Co2-Bp-C*/2 were verified for OspC expression by immunoblot probed with a mixture of FlaB and OspC MAbs.

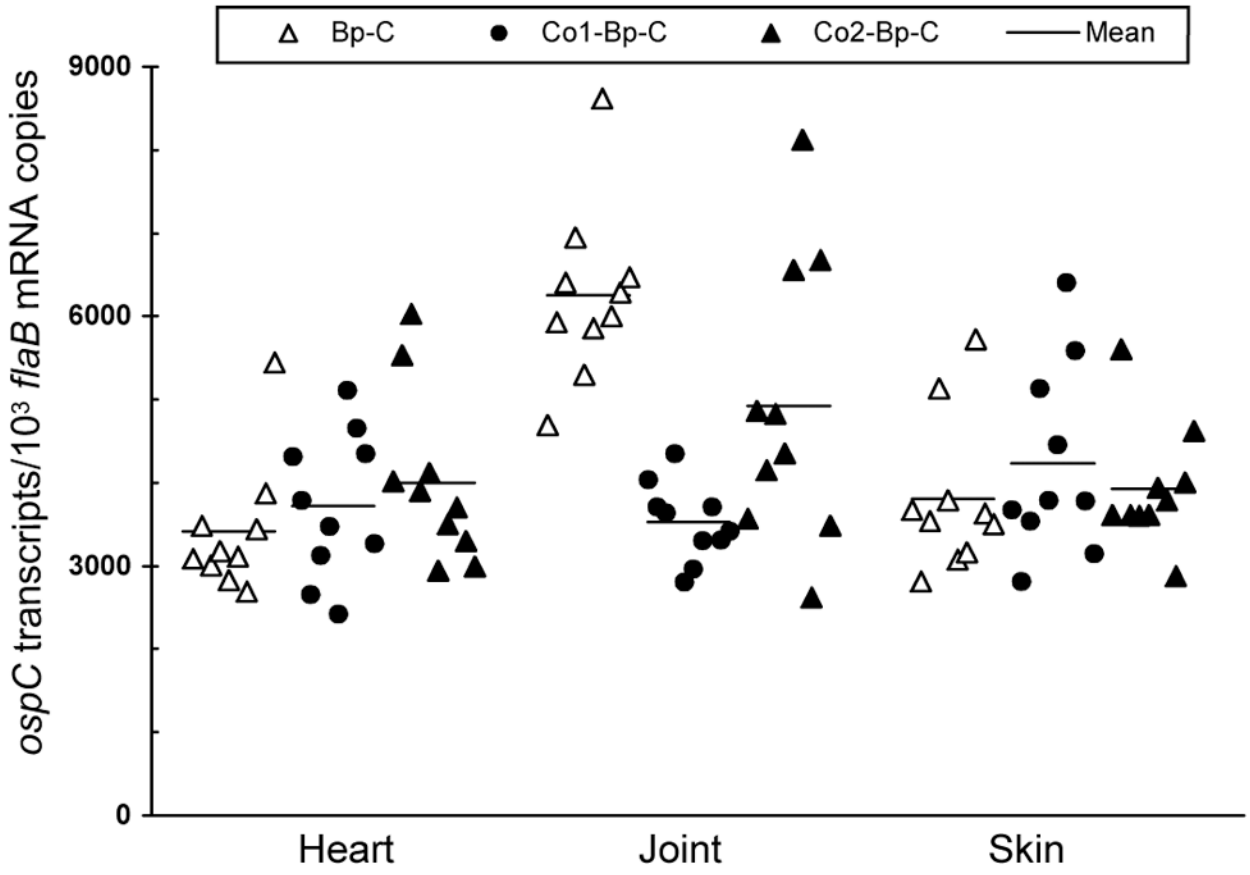

Fig. 4.

The long *ospC* operator version more effectively reduces the activity of a fused *flaB* promoter in joints of SCID mice. Subgroups of five SCID mice were inoculated with the clone *Bp-C*/1, *Bp-C*/2, *Co1-Bp-C*/1, *Co1-Bp-C*/2, *Co2-Bp-C*/1 or *Co2-Bp-C*/2. One month later, mice were euthanized; heart, joint and skin specimens were used for RNA extraction. RNA samples were quantified for *flaB* and *ospC* expression by RT-qPCR. Data are presented as *ospC* transcripts per 1000 *flaB* mRNA copy numbers in three groups by combining the subgroups *Bp-C*/1 and *Bp-C*/2, *Co1-Bp-C*/1 and *Co1-Bp-C*/2, and *Co2-Bp-C*/1 and *Co2-Bp-C*/2.

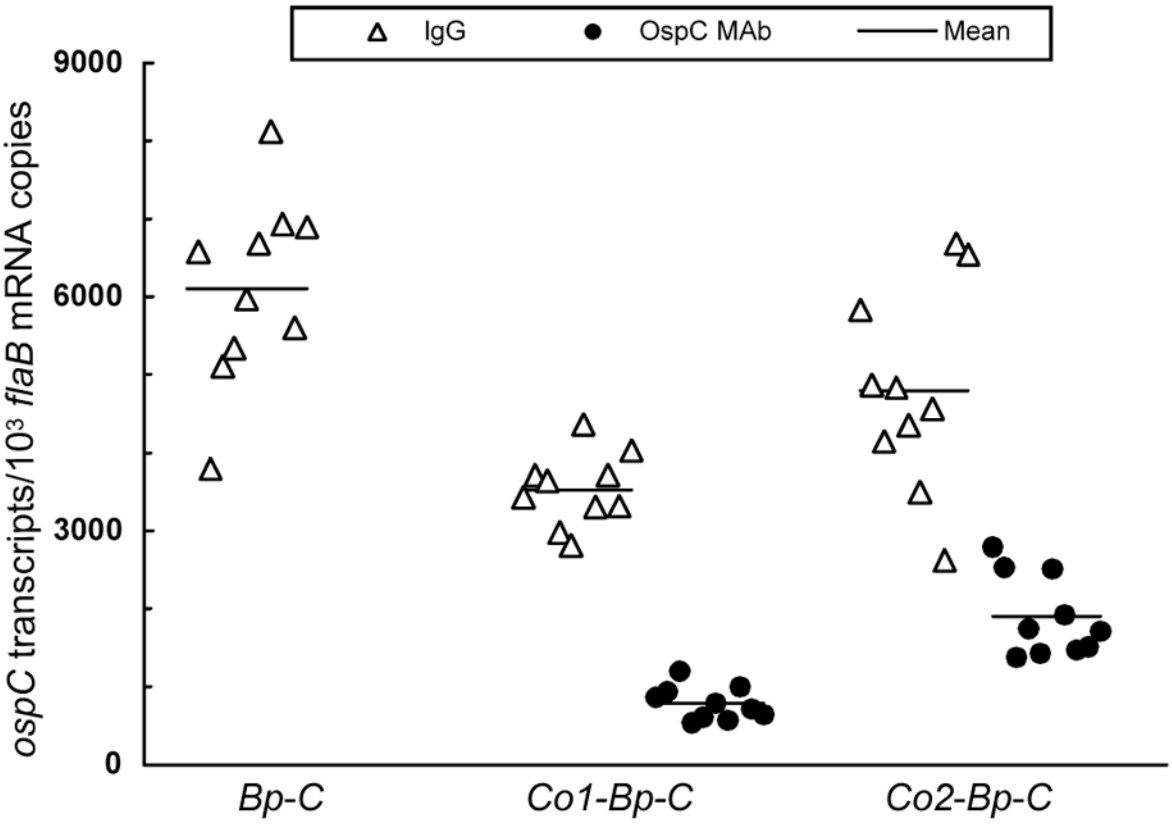

Fig. 5.

The long *ospC* operator version more effectively reduces the activity of a fused *flaB* promoter in response to treatment with OspC MAb. Subgroups of 10 SCID mice were inoculated with the clone *Bp-C*/1, *Bp-C*/2, *Co1-Bp-C*/1, *Co1-Bp-C*/2, *Co2-Bp-C*/1 or *Co2-Bp-C*/2. Three weeks later, five mice from each subgroup received a single dose of 100 μg of either OspC MAb or purified murine IgG as a control. One week later, mice were euthanized; RNA was extracted from joint specimens harvested from the 30 IgG-treated mice and from the 20 mice infected with the *Co1-Bp-*/1, *Co1-Bp-C*/2, *Co2-Bp-C*/1, or *Co2-Bp-C*/2 bacteria and treated with OspC MAb. RNA samples were quantified for *flaB* and *ospC* expression by RT-qPCR. Data are presented as *ospC* transcripts per 1000 *flaB* mRNA copies in three groups by combining the subgroups *Bp-C*/1 and *Bp-C*/2, *Co1-Bp-C*/1 and *Co1-Bp-C*/2, and *Co2-Bp-C*/1 and *Co2-Bp-C*/2. The *Bp-C*/1 and *Bp-C*/2 bacteria were cleared by OspC MAb; therefore no expression data were obtained from this treatment.

Table 1

Constructs and clones used in the study

Construct or clone	Description	Source
pBBE22	pBSV2 carrying a *bbe22* copy	[39]
pBBE22-*ospC′*	pBBE22 carrying promoterless *ospC* fused with long version of *flaB* promoter	[20]
pBBE22-*flaBp*$_{min}$-*ospC*	pBBE22 carrying promoterless *ospC* fused with minimal *flaB* promoter	This study
pBBE22-*Co1-flaBp-ospC*	pBBE22 carrying promoterless *ospC* fused with minimal *flaB* promoter which is fused with long version of *ospC* operator	This study
pBBE22-*Co2-flaBp-ospC*	pBBE22 carrying promoterless *ospC* fused with minimal *flaB* promoter which is fused with short version of *ospC* operator	This study
ΔospC	*ospC* mutant	[34]
ΔospC/*FL*/1	Expressing *ospC* controlled by *ospC* regulatory elements[a]	[34]
ΔospC/*ospC′*/1	Expressing *ospC* driven by long version of *flaB* promoter	This study
ΔospC/*ospC′*/2	Expressing *ospC* driven by long version of *flaB* promoter	This study
Bp-C/1	Expressing *ospC* driven by minimal *flaB* promoter	This study
Bp-C/2	Expressing *ospC* driven by minimal *flaB* promoter	This study
Co1-Bp-C/1	Expressing *ospC* driven by minimal *flaB* promoter which is controlled by long version of *ospC* operator	This study
Co1-Bp-C/2	Expressing *ospC* driven by minimal *flaB* promoter which is controlled by long version of *ospC* operator	This study
Co2-Bp-C/1	Expressing *ospC* driven by minimal *flaB* promoter which is controlled by short version of *ospC* operator	This study
Co2-Bp-C/2	Expressing *ospC* driven by minimal *flaB* promoter which is controlled by short version of *ospC* operator	This study

[a]The *ospC* regulatory elements include both operator and promoter.

Table 2

The *ospC* operator helps *B. burgdorferi* evade clearance by OspC MAb[a]

Clone	Treatment received	No. of cultures positive/Total no. of specimens examined			
		Heart	Joint	Skin	All sites
ΔospC/FL/1	mouse IgG	5/5	5/5	5/5	15/15
	OspC MAb	3/5	5/5	4/5	12/15
Bp-C/1	mouse IgG	5/5	5/5	5/5	15/15
	OspC MAb	0/5	0/5	0/5	0/15
Bp-C/2	mouse IgG	5/5	5/5	5/5	15/15
	OspC MAb	0/5	0/5	0/5	0/15
Co1-Bp-C/1	mouse IgG	5/5	5/5	5/5	15/15
	OspC MAb	0/5	5/5	3/5	8/15
Co1-Bp-C/2	mouse IgG	5/5	5/5	5/5	15/15
	OspC MAb	0/5	5/5	3/5	8/15
Co2-Bp-C/1	mouse IgG	5/5	5/5	5/5	15/15
	OspC MAb	0/5	5/5	2/5	7/15
Co2-Bp-C/2	mouse IgG	5/5	5/5	5/5	15/15
	OspC MAb	0/5	5/5	3/5	8/15

[a]Groups of 10 BALB/c SCID mice were inoculated with the clone *ΔospC/FL*/1, *Bp-C*/1, *Bp-C*/2, *Co1-Bp-C*/1, *Co1-Bp-C*/2, *Co2-Bp-C*/1 or *Co2-Bp-C*/2. Three weeks later, five animals from each group received a single dose of either OspC MAb or murine IgG as a control and were sacrificed within 1 week. Heart, tibiotarsal joint and skin specimens were harvested and cultured for spirochetes in BSK-H complete medium.

Table 3

The *ospC* operator facilitates immune evasion of *B. burgdorferi*[a]

Clone	No. of cultures positive/Total no. of specimens examined			
	Heart	**Joint**	**Skin**	**All sites**
ΔospC/*FL*/1	10/10	10/10	10/10	30/30
Bp-C/1	0/5	0/5	3/5	3/15
Bp-C/2	0/5	0/5	4/5	4/15
Co1-Bp-C/1	3/5	5/5	5/5	13/15
Co1-Bp-C/2	3/5	4/5	5/5	12/15
Co2-Bp-C/1	4/5	2/5	5/5	11/15
Co2-Bp-C/2	4/5	3/5	5/5	12/15

[a] Groups of five or 10 BALB/c mice were inoculated with the clone *ΔospC*/*FL*/1, *Bp-C*/1, *Bp-C*/2, *Co1-Bp-C*/1, *Co1-Bp-C*/2, *Co2-Bp-C*/1 or *Co2-Bp-C*/2. Mice were sacrificed 4 months post-inoculation. Heart, tibiotarsal joint and skin specimens were harvested and cultured for spirochetes in BSK-H complete medium. Fisher's exact test *P* values were 0.01 and 1.2×10^{-4} between the genotypes *Bp-C* and *Co1-Bp-C* in heart and joint tissues, 7.1×10^{-4} and 0.03 between *Bp-C* and *Co2-Bp-C* in heart and joint tissues, and 0.63 and 0.14 between *Co1-Bp-C* and *Co2-Bp-C* in heart and joint tissues, respectively.

Table 4

Primers used in this study

Primer name	Primer sequence (5′ to 3′)[a]
P1F	TAGGATCCTTCTTTTTTTTTAATTTTTGTGCTA
P1R	TTCCTCTAGAGAAGAGCTTAAAGTTAA
P2F	TAGTTGGCTATATTGGGATCCAA
P2R	CAGAGAATTCTTTATTTGAAAAAATAATTTTTTC
P3F	ACAGGAATTCTTTTTTTTTAATTTTTGTGCTATTCT
P3R	TTGAATTCTTTTTCAAATTCTTCAATATCTTGA
P4F	TTGGGATCCAAAATCTAATACAAGT
P4R	GGAAATCTTCCTTGAAGCT
P5F	GCAGCTAATGTTGCAAATCTTTTC
P5R	GCAGGTGCTGGCTGTTGA
P6F	ATGCCTCTTCCGACCATCAAGCA
P6R	GATCGCAGTGGTGAGTAACCATGCA

[a]The underlined sequences are restriction enzyme sites: *Bam*HI sites (P1F and P4F), a *Xba*I site (P1R), and *Eco*RI sites (P2R, P3F and P3R).